A Self-referenced VCO-based Temperature Sensor with 0.034°C/mV Supply Sensitivity in 65nm CMOS

Tejasvi Anand, Kofi A.A. Makinwa* and Pavan Kumar Hanumolu
University of Illinois, Urbana-Champaign, IL, USA, *Delft University of Technology, Delft, Netherlands
E-mail: tanand3@illinois.edu

Abstract

A VCO-based temperature sensor with low supply sensitivity is presented. Fabricated in a 65nm CMOS process, the 0.004mm^2 prototype operates with 1V supply and achieves a supply sensitivity of 0.034°C/mV and an inaccuracy of +0.9°C/- 0.9°C and +2.3°C/-2.3°C from 0-100°C after 2-point calibration, with and without static non-linearity correction, respectively. For (programmable) resolutions of 1°C-to-0.3°C, the sensor draws 1nJ-to-3.4nJ per conversion, respectively.

Introduction

Modern microprocessors utilize several on-chip temperature sensors for thermal monitoring [1]. Such sensors must be placed close to hotspots, which mandates small area, scalability with process, and immunity to supply voltage variations, as they should run off the digital power supply [2]. Furthermore, the use of external bias and clock circuitry should be avoided. To meet these challenges, several all-CMOS sensor architectures have been proposed. DTMOST based sensors [3] offer high accuracy, low power and sub-1V operation, but occupy large area. Delay based sensors employing TDC and DLL architectures offer small size and scale well with process. However, their need for reference clocks [4], operational amplifiers [5] and voltage regulators [6], hinder their usage in microprocessors. In view of these drawbacks, we present a VCO-based self-referenced sensor with digital readout, reduced supply sensitivity and small size.

Concept and Architecture

The operation of the proposed temperature sensor is illustrated in Fig. 1. It is based on the observation that a ring oscillator's frequency has a CTAT characteristic due to the mobility-dominated temperature dependence of its inverters (at the nominal supply voltage of a 65nm process). However, the exact slope of this characteristic is a function of the threshold voltages V_{TH} of the transistors used in the inverters (Fig. 1(a)). Temperature can then be estimated from the ratio of the frequencies of two different ring oscillators VCO1 and VCO2, each employing transistors with different threshold voltages. As shown in Fig. 1(b), this estimate has a PTAT characteristic. The difference in threshold voltages is realized by exploiting the variation of V_{TH} with channel length (Fig. 1(c)). Increasing the length of the MOSFETs in VCO2 relative to those in VCO1 results in a steeper CTAT characteristic (Fig. 1(a)). The sensor's temperature dependence is thus mainly determined by layout, rather than by the use of additional analog components.

A drawback of ring oscillators is their supply sensitivity. An expression for the temperature estimate F_{VCO1}/F_{VCO2} is given in Fig. 2. The first term increases with V_{DD}, while the second term is the ratio of the load capacitances C_{L1} and C_{L2} of VCO1 and VCO2, respectively. Each C_L consists of wire capacitance, gate capacitance and drain-bulk junction capacitance C_{DB}. However, the latter decreases as V_{DD} increases, since the depletion width of the p-n junction formed between bulk and drain increases. By ensuring that C_{L2} is dominated by C_{DB}, the ratio of the two

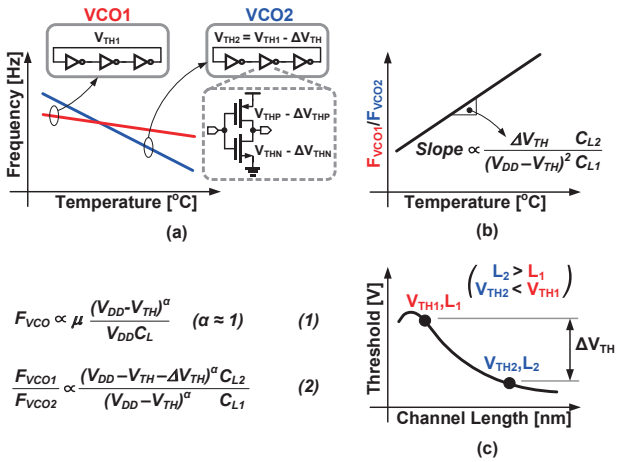

Fig. 1: Operating principle of the proposed VCO based sensor.

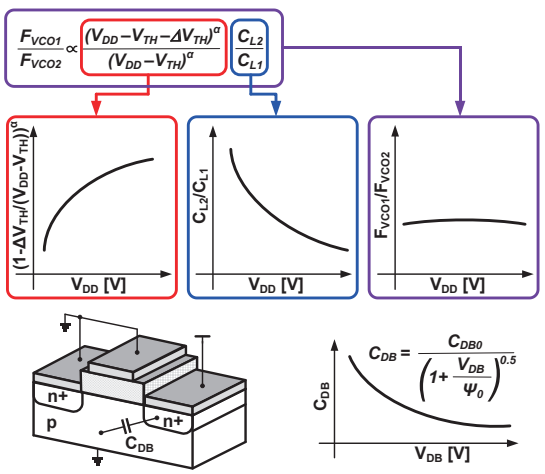

Fig. 2: Proposed concept of reducing supply sensitivity.

load capacitances, C_{L2}/C_{L1} can be made to decrease with V_{DD}. The sensor's supply sensitivity can then be significantly reduced by properly balancing the first and second terms of the F_{VCO1}/F_{VCO2} ratio.

The architecture of the proposed sensor is shown in Fig. 3. It consists of VCO1 and VCO2, which clock two programmable counters Counter1 and Counter2, respectively, and a state machine. The state machine is clocked by VCO2 and generates control signals to latch and reset the counters. As explained above C_{L2} is dominated by C_{DB}, length of VCO2 MOSFETs is longer than that in VCO1 and so F_{VCO1} is about 4x higher than F_{VCO2}. When Counter2 reaches a predetermined threshold count, the value of Counter1 is latched, which represents die temperature (F_{VCO1}/F_{VCO2}). Thereafter, both the counters are reset to zero and the sequence begins again. Temperature sensor quantization error can be programmed by adjusting the threshold of Counter2. Simulations show that the ratio F_{VCO1}/F_{VCO2} exhibits a static non-linearity. This can be corrected with a second order polynomial whose coefficients are kept constant for the entire fabricated lot.

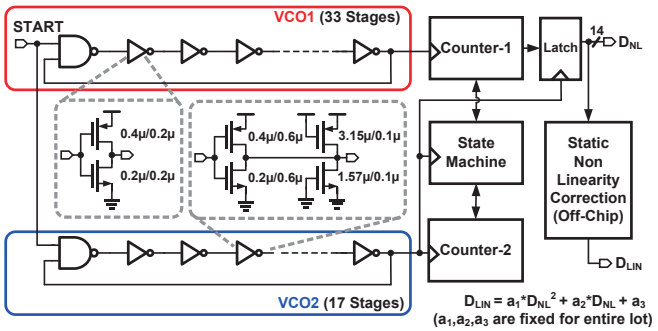

Fig. 3: Simplified architecture of the proposed temperature sensor.

Measurement Results

The prototype temperature sensor is fabricated in a 65nm CMOS logic process and has an active area of 0.004mm^2. Operating from a 1V supply, it consumes a total power of 154μW, of which 60μW is consumed by the VCOs and the remaining by the digital logic (Fig. 4(b)). Fig. 4(a) shows the measured inaccuracy of 7 test chips after 2-point calibration and with and without static non-linearity correction. The sensor achieves an inaccuracy of +0.9°C/-0.9°C over a temperature range of 0-100°C.

Fig. 5 shows the measured supply and temperature sensitivity of VCO1 and VCO2. For a supply range of 0.75V-to-1.1V, F_{VCO1} and F_{VCO2} change at a rate of 1514ppm/mV and 1500ppm/mV, respectively. For the 0-100°C temperature range, F_{VCO1} and F_{VCO2} change at a rate of -1640ppm/°C and -2260ppm/°C, respectively. The supply sensitivities of VCO1 and VCO2 are thus quite similar, unlike their temperature sensitivities. Fig. 6 shows the measured supply sensitivity of 7 test chips at 30°C and 70°C. The peak-peak supply sensitivity is then about 0.032°C/mV and 0.037°C/mV, respectively.

The sensor's resolution is determined by measuring the amount of noise in its output. Fig. 7(a) shows a histogram of 100 measurements at 0°C and 100°C, which have standard deviations of 0.3°C and 0.2°C, respectively. A die micrograph is shown in Fig. 7(b). Fig. 8 summarizes the sensor's performance and compares it with the state-of-the-art. Without using external clock references, supply regulators, operational amplifiers or bias circuitry, the proposed sensor achieves competitive accuracy and area with a highly scalable, portable and robust VCO-based architecture.

Acknowledgments

This work was in part supported by Analog Devices and by the NSF CAREER award EECS-0954969. We thank Berkeley Design Automation for providing Analog Fast Spice (AFS) simulator and Seong Joong Kim for help in testing.

References

[1] M. Floyd, *et al*., *Micro*, vol. 31, no. 2 pp. 60–75, 2011.
[2] Y. William Li, *et al*., *CICC,* pp. 1–8, Sep. 2011.
[3] K. Souri, *et al*., *ISSCC,* pp. 222–223, Feb 2014.
[4] E. Saneyoshi, *et al*., *Symp. VLSI*, pp. 152–153, June 2008.
[5] S. Jeong, *et al., JSSC,* vol. 49, no. 8, pp. 1682–1693, 2014.
[6] S. Hwang, *et al., TCAS-I,* vol. 60, no. 9, pp. 2241–2248, 2013.

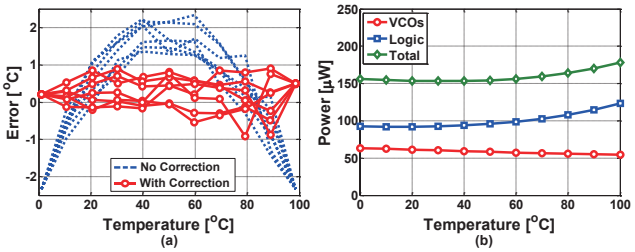

Fig. 4: a) Measured inaccuracy of 7 test chips with 2-point trimming, w/ and w/o nonlinearity correction. b) Sensor's power breakdown.

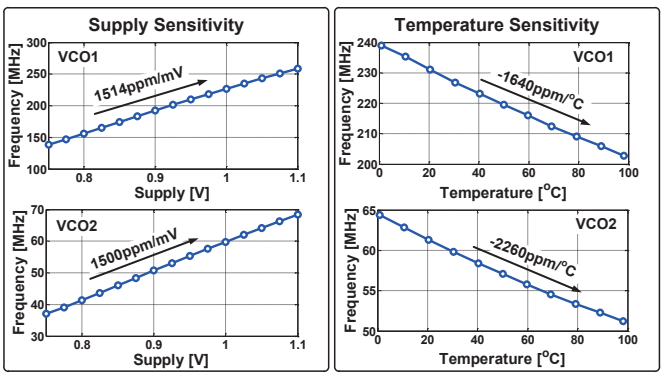

Fig. 5: Measured supply and temperature sensitivity of the VCOs.

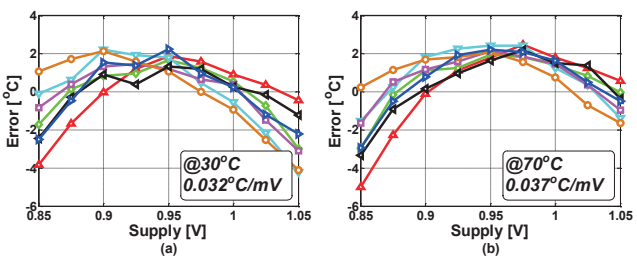

Fig. 6: Measured supply sensitivity of 7 test chips at 30°C and 70°C.

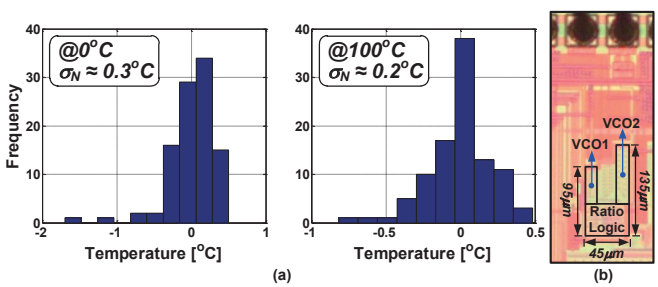

Fig. 7: a) Measured histogram of 100 sensor readings at 0°C and 100°C. b) Die micrograph of the temperature sensor.

	This Work	JSSC'14 [5]	ISSCC'14 [3]	TCAS-I'13 [6]	VLSI'08 [4]
Technology	65nm	180nm	160nm	65nm	65nm
Type	MOSFET	MOSFET	DTMOST	MOSFET	MOSFET
Area [mm^2]	0.004mm^2	0.09mm^2	0.085mm^2	0.008mm^2	0.0012mm^2
Supply [V]	0.85-1.05	1.2	0.85-1.2	1	1.1
External Clock Reference	NO	NO	NO	NO	YES
Supply Regulator	NO	NO	NO	YES	NO
Temperature Range [°C]	0-100°C	0-100°C	-40-125°C	0-110°C	0-100°C
Resolution [°C]	0.3°C-to-1°C	0.3°C	0.063°C	0.18°C	1°C
Conversion Time [s]	22μs-to-6.5μs	30ms	6ms	2.1μs	1ms
Calibration	2-point	2-point	1-point	1-point	NA
Inaccuracy [°C] (w/ and w/o correction)	+0.9°C/-0.9°C +2.3°C/-2.3°C	+1.5°C/-1.4°C	+0.4°C/-0.4°C	+1.5°C/-1.5°C	3.1°C
Power	154μW@1V	71nW	600nW	500μW	NA
Energy/Conversion [nJ]	3.4nJ-to-1nJ	2.2nJ	3.6nJ	1nJ	NA
Supply Sensitivity [°C/mV]	0.034°C/mV	0.014°C/mV	0.00045°C/mV	(regulated)	0.02°C/mV

Fig. 8: Performance summary and comparison with state-of-the-art.